Heliyon 10 (2024) e24210

Contents lists available at ScienceDirect

Heliyon

journal homepage: www.cell.com/heliyon

Research article

The physicochemical properties and molecular docking study of plasticized amphotericin B loaded sodium alginate, carboxymethyl cellulose, and gelatin-based films

Saurabh Bhatia [a,b,c,*,1], Ahmed Al-Harrasi [a,**,1], Ibrahim Hamza Almohana [d], Mustafa Safa Albayati [d], Muhammad Jawad [a], Yasir Abbas Shah [a], Sana Ullah [a], Anil K. Philip [d], Sobia Ahsan Halim [a,***], Ajmal Khan [a], Md Khalid Anwer [e], Esra Koca [f], Levent Yurdaer Aydemir [f], Sevgin Dıblan [g]

[a] Natural and Medical Sciences Research Center, University of Nizwa, P.O. Box 33, Birkat Al Mauz, Nizwa, 616, Oman
[b] School of Health Science, University of Petroleum and Energy Studies, Dehradun, 248007, India
[c] Saveetha Institute of Medical and Technical Sciences, Saveetha University, Chennai, 600077, India
[d] School of Pharmacy, College of Health Sciences, University of Nizwa-616, Birkat Al Mouz, Oman
[e] Department of Pharmaceutics, College of Pharmacy, Prince Sattam Bin Abdulaziz University, Al-Kharj, 11942, Saudi Arabia
[f] Department of Food Engineering, Adana Alparslan Turkes Science and Technology University, 01250, Adana, Turkey
[g] Food Processing Department, Vocational School of Technical Sciences at Mersin Tarsus Organized Industrial Zone, Tarsus University, 33100, Tarsus/Mersin, Turkey

ARTICLE INFO

Keywords:
Amphotericin B
Sodium alginate
Glycerol
Carboxymethyl cellulose
Gelatin
Bioadhesive films
Topical

ABSTRACT

Plasticizers are employed to stabilize films by safeguarding their physical stability and avoiding the degradation of the loaded therapeutic drug during processing and storage. In the present study, the plasticizer effect (glycerol) was studied on bioadhesive films based on sodium alginate (SA), carboxymethyl cellulose (CMC) and gelatin (GE) polymers loaded with amphotericin B (AmB). The main objective of the current study was to assess the morphological, mechanical, thermal, optical, and barrier properties of the films as a function of glycerol (Gly) concentration (0.5–1.5 %) using different techniques such as Scanning Electron Microscope (SEM), Texture analyzer (TA), Differential Scanning Calorimeter (DSC), X-Ray Diffraction (XRD), and Fourier Transforms Infrared Spectroscopy (FTIR). The concentration increase of glycerol resulted in an increase in Water Vapor Permeability (WVP) (0.187–0.334), elongation at break (EAB) (0.88–35.48 %), thickness (0.032–0.065 mm) and moisture level (17.5–41.76 %) whereas opacity, tensile strength (TS) (16.81–0.86 MPa), and young's modulus (YM) (0.194–0.002 MPa) values decreased. Glycerol incorporation in the film-Forming solution decreased the brittleness and fragility of the films. Fourier Transform Infrared (FTIR) spectra showed that intermolecular hydrogen bonding occurred between glycerol and polymers in plasticized films compared to control films. Furthermore, molecular docking was applied to predict the binding interactions betweem AmB, CMC, gelatin, SA and glycerol, which further endorsed the stabilizing effects of glycerol in the complex formation between AmB, CMC, SA, and gelatin. The Findings of the

* Corresponding author. Natural and Medical Sciences Research Center, University of Nizwa, P.O. Box 33, Birkat Al Mauz, Nizwa, 616, Oman.
** Corresponding author.
*** Natural and Medical Sciences Research Center, University of Nizwa, P.O. Box 33, Birkat Al Mauz, Nizwa 616, Oman.
E-mail addresses: sbsaurabhbhatia@gmail.com (S. Bhatia), aharrasi@unizwa.edu.om (A. Al-Harrasi), sobia_halim@unizwa.edu.om (S.A. Halim).
[1] These authors contributed equally to this work.

https://doi.org/10.1016/j.heliyon.2024.e24210
Received 17 August 2023; Received in revised form 21 December 2023; Accepted 4 January 2024
Available online 14 January 2024

current study demonstrated that this polymeric blend could be used to successfully prepare bioadhesive films with glycerol as a plasticizer.

1. Introduction

Fungal infection is usually present over the sites such as the skin, throat, stomach, etc. Once this infection propagates in the human body it can cause significant mortality and morbidity, particularly in immunocompromised patients. A recent report showed that fungal infections caused almost 1.7 million deaths annually [1]. There are various therapeutics available and are under development against fungal infections that have primary concerns related to toxicity, resistance, efficacy, bioavailability, mechanism of action, antifungal spectrum, etc [2]. Amphotericin B (AmB) is a broad-spectrum antifungal belonging to a class of polyenes and is primarily used for the treatment of invasive fungal infections, and is known to be amphoteric [3]. This life-saving drug is mainly used for mycosis by acting on ergosterol, a steroid present in the membranes of fungal cells. AmB has poor bioavailability and causes adverse reactions when administered in parenteral mode. In addition to parenteral preparations, oral preparations of AmB can cause several side effects and toxicity. For these reasons lipid-based formulations such as AmBisome, Amphotec and Abelcet have been developed; however, their use is compromised owing to side effects and high cost [4].

Recently conducted studies have revealed a growing significance of the development of topical formulations that may improve drug penetration into the skin. Nevertheless, topical administration of AmB in formulations such as gel, lotion, or cream could limit its therapeutic effectiveness, cause dose variation, and other problems. Moreover, these liquid and semisolid-based formulations have stability issues, cause irritation to the skin, are incompatible with skin secretions, and are messy in nature. Furthermore, the low drug loading capacity, various side effects, and high cost of these formulations limit their application. The studies have exhibited an interest in the development of bioadhesive films. Bioadhesive films can offer intimate contact with the films at the target site, enhance the residence period, and in this manner offer proper drug release attributes. Thus, the present study aimed to develop a stable AmB-loaded topical bioadhesive preparation based on sodium alginate (SA), Gelatin (GE), and Carboxymethyl Cellulose (CMC). SA (anionic) and GE (cationic) are natural water-soluble, non-toxic, and biodegradable polymers. It has been extensively used for several pharmaceutical and biomedical applications [5]. Nevertheless, because of their lower cellular adhesion, they should be mixed with other hydrophilic polymers with bioadhesive properties, namely CMC.

CMC is a safe, non-toxic, hydrosoluble, biocompatible bioadhesive, and biodegradable cellulose derivative that can be used in the design of topical drug delivery systems. This polymer is generally recognized as safe and is frequently used as a composite with other polymers to suppress its swelling behavior and impart bioadhesion properties [6]. AmB is a BCS class IV drug with low permeability and solubility. Thus, it is important to improve drug permeation via the skin, using permeation enhancers such as surfactants (Tween 80, sodium laurylsulphate, alkyl dimethylbenzyl ammonium halides, etc.) [7]. In this study, surfactants such as Tween 80 were used as chemical penetration enhancers.

The research objective of this study was to engineer advanced topical Amphotericin B (AmB) formulations by employing natural polymers such as SA, GE, and CMC, with the incorporation of glycerol (Gly) serving as a plasticizer, to significantly improve the physicochemical properties of the formulations. Therefore, the aim of this research was to explore the impact of glycerol on the morphological and physical characteristics and study the interactions at a molecular level among different components in composite materials.

2. Materials and methods

2.1. Materials and film preparation

Gelatin ex. Porcine (120 g Bloom Type B), Sodium alginate (SA), Carboxymethyl cellulose (CMC), Amphotericin B (b.no. 5349691), and Tween 80 were purchased from Sisco Research Laboratories Pvt Ltd., Mumbai, India. BDH Laboratory (London, England) provided the glycerol (Gly) used in this study.

The casting method was employed for the preparation of the bioadhesive film using SA, GE and CMC as polymers, Gly as a plasticizer, and Tween 80 as a permeation enhancer. The composition of the formulation is presented in Table 1. The film-forming solutions (FFSs) of each polymer i.e., SA (1.05 % (w/v)), GE (0.45 % (w/v)) and CMC (0.75 % (w/v)) were prepared by dissolving each polymer in distilled water separately. All polymeric dispersions were mixed by using the magnetic stirrer for 1 h. After 1 h of mixing, one fourth part of the solution was separated and labeled as blank (S1). Later, AmB (0.1 %) was added to the resultant solution

Table 1
Composition of the blank (S1) and AmB/Gly loaded films (S2–S4).

Codes	SA (w/v)	GE (w/v)	CMC (w/v)	Gly(v/v)	AmB (w/v)
S1	1.05 %	0.45 %	0.75 %	–	–
S2	1.05 %	0.45 %	0.75 %	0.5 %	0.1 %
S3	1.05 %	0.45 %	0.75 %	1 %	0.1 %
S4	1.05 %	0.45 %	0.75 %	1.5 %	0.1 %

and mixed using the magnetic stirrer for 1 h. The solution was further divided into three beakers labeled S2, S3, and S4. Different concentrations of Gly (v/v) (0.5, 1 %, 1.5 %) were added to respective S2, S3, and S4 samples. Table 1 details the composition of the FFS in the current study. The polymeric solutions obtained after mixing for 3 h were transferred into coded petri plates (90 mm × 15.8 mm) and subjected to drying for 48 h at room temperature. Subsequently, the films were carefully peeled off the petri plates for visual assessment and later kept in a desiccator (24 h at 25 °C) before further analysis.

2.2. Film thickness assessment

The determination of the thickness of the prepared films helps to determine the optimal bio adhesion and ensures uniformity of content. The film thickness of AmB-loaded SA–GE films were assessed by using a thickness analyzer (Mitutoyo digital micrometer 2046F, Mitutoyo, Kawasaki, Japan). Five points were randomly selected from each film (n = 5), and the average was calculated.

2.3. Mechanical characterization of the bioadhesive films

The mechanical characterization of the films is an important parameter to assess the durability of films. Films with cracks, pores, and bubbles were not included. Preconditioning of the samples was carried out at 50 % relative humidity for a period of at least 40 h at 25 °C in a test cabinet (Nüve TK 120, Türkiye) before analysis. In this method (ASTM D882, 2010), rectangular strips were prepared with dimensions of 7 mm × 70 mm and placed between two clamps at 60 mm distance. The mechanical parameters such as TS, EAB and YM were calculated by using equations (1)–(3) respectively.

$$TS = \left(\frac{F}{A}\right) \tag{1}$$

where, F = force and A = film's cross-sectional area.

$$EAB\ (\%) = \frac{Lf - Li}{Li} \times 100 \tag{2}$$

where Li = film's initial length and Lf = final length at a break.

$$YM = \left(\frac{Stress}{Strain}\right) \tag{3}$$

2.4. Moisture content (MC)

The gravimetric procedure was employed to assess the proportion of moisture content in the films. In gravimetric analysis, the samples were subjected to drying (105 °C) and weight difference (before and after) was assessed using equation (4).

$$MC = \frac{W1 - W2}{W1} \times 100 \tag{4}$$

W1 = initial weight, and W2 = Final weight.

2.5. Assessment of water solubility

To assess the solubility in water Kim and Song [8] procedure was followed. In this procedure, the samples were dried at 105 °C, and weight was calculated as W1. The films were submerged in distilled water (20 ml) and placed in the incubator for mixing for 24 h. Finally, the films were dried in the hot air oven at 105 °C, and the weight of each film was determined as W2. Equation (5) was used to assess the water solubility of the sample.

$$WS = \frac{W1 - W2}{W1} \times 100 \tag{5}$$

W1 = initial weight, and W2 = Final weight.

2.6. Water Vapor Permeability (WVP) of the films

The procedure described by Erdem et al. was employed to calculate the WVP of the film samples [9]. Initially, the samples were placed in the desiccator where relative humidity was reduced to 50 %. During this method, glass cups with dimensions of 5 × 3 cm were used. Later, the relative humidity (RH) of the glass cups was maintained by using silica gel (RH 0 %) and water (RH 100 %). To assess the weight variation, silica gel-containing glass cups were wrapped with films and tightly sealed. This is followed by the measurement of the weight of the cups on an hourly basis. Equation (6) was used to calculate WVP.

$$WVP = \frac{\Delta m}{\Delta t \times \Delta P \times A} \times d \tag{6}$$

$\Delta m/\Delta t$ = gain in moisture content per unit of time (g/d); A = area of the film (m^2); ΔP = variation in the water vapor pressure between both sides of the film (kPa), and d = film thickness.

2.7. Color and transparency assessment

Color analysis of the films is an important attribute that determines film appearance and end consumer acceptability. Konica Minolta Colorimeter (Tokyo, Japan) was employed for the measurement of the color parameters of the samples. CIELAB color scale and overall color variation were measured using Equation (7), where a* represents red–green and b* represents yellow–blue parameters with respect to a reference plate (L* = 100).

$$\Delta E* = \left[(\Delta L^*)^2 + (\Delta a^*)^2 + (\Delta b^*)^2\right]^{\frac{1}{2}} \tag{7}$$

ΔE = overall color difference.

Films transparency was measured by spectrophotometer, as per the procedure described by Zhao et al. [10]. To evaluate the transparency, the ONDA-Vis spectrophotometer (Model V-10 Plus, manufactured by ONDA, Italy) was calibrated to a wavelength of 550 nm. Subsequently, the absorbance levels of the rectangular film samples were measured using this setting. Four measurements were obtained for each sample and equation (8) was employed to assess films transmittance:

$$\%T = 10^{(2-A)} \tag{8}$$

%T represents percent transmittance, A is the absorbance of light.

2.8. Differential scanning calorimetry

The Differential Scanning Calorimetry (DSC) analysis was conducted using a DSC-Q20 device (produced by TA Instruments, New Castle, DE, USA). A sample of the film, weighing 5–10 mg, was securely sealed in aluminum pans and then positioned in the instrument's sampling area. The samples underwent a heating process (25 °C–200 °C at a rate of 10 °C per min) in an environment enriched with nitrogen at a constant purge flow.

2.9. Antimicrobial assay of AMB loaded films

The agar diffusion method from Seol et al.[11] and Matuschek et al.[12] was used to assess the antimicrobial activity of the films with minor modification. A yeast *Candida albicans* (ATCC 10231) were used to challenge bacterial cells to determine antimicrobial efficacy since amphotericin B is antifungal. Before analysis, *C. albicans* was activated using tryptic soy agar (TSA) by incubating at 35 °C for 18 h. After activation, the suspension was prepared in sterile saline solution (0.85 % w/v NaCl) with a 0.5 McFarland turbidity level. A suspension containing *C. albicans* was spread well onto Mueller–Hinton agar using cotton swap at 0.5 McFarland turbidity standards (~10^8 CFU/ml). The films were cut in 10 mm diameter and placed onto Mueller–Hinton agar inoculated with targeted strains. The films do not have any antimicrobial agent used as negative controls. The plates were incubated at 35 °C for 24–48 h. The diameters of the inhibitory halo zones were measured in millimeters in different parts zones, and the results were averaged.

2.10. XRD analysis

An X-ray diffractometer (Bruker D8 Discover instrument) was used to assess the extent of crystallinity of films and the instrument was adjusted at the 2θ (theta) ranging from 5° to 50°(40 kV).

2.11. SEM analysis

The surface morphology and cross-section of the films were investigated by SEM (JSM6510LA from Analytical SEM, Jeol, Japan). Gold coating was performed to make the films conductive before taking images.

2.12. FTIR analysis

The bioadhesive films were analyzed by FTIR (InfraRed Bruker Tensor 37, Ettlingen, Germany) to study the interaction between polymers, drugs, plasticizer, and surfactant. The obtained spectra were recorded in the range of range 400–4000 cm^{-1}, with an average of 32 scans at 25 °C.

2.13. In-vitro drug release studies

The *in-vitro* drug release analysis (n = 6) was conducted using a USP dissolution test apparatus I (basket apparatus) with 500 ml of simulated saliva (pH 6.8) maintained at 37 ± 0.5 °C and agitated at a rate of 50 rpm. The film was sliced into a 2 × 2 cm^2 patch, put inside the basket, and submerged in the USP apparatus filled with the dissolution medium. Samples of 5 ml were extracted (by using a filter paper at the tip of the pipette) at time intervals of 0, 5, 10, 15, 20, and 40 min, and examined using UV–visible spectrophotometry

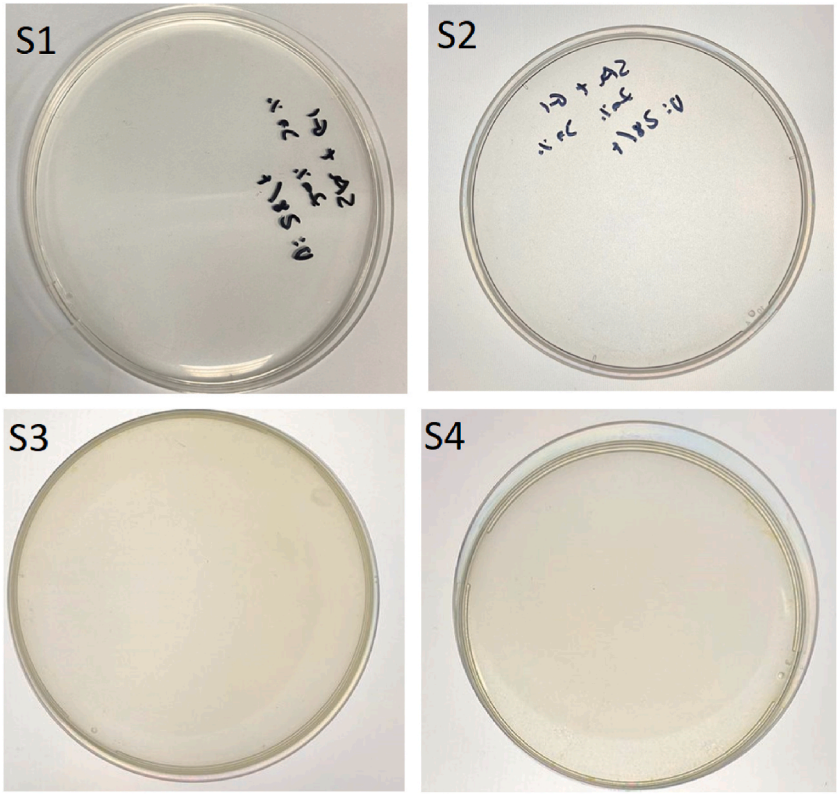

Fig. 1. Visual assessment of the bioadhesive films from S1–S4. Film-S1: control film (no Gly), Film-S2: Gly (0.5 % v/v) film, Film-S3: Gly (1 % v/v) film, and Film-S4: Gly (1.5 % v/v) film.

at a wavelength of 328 nm.

2.14. *In-vitro bioadhesion time*

The time for *in-vitro* bioadhesion of various films was observed by assessing the number of times the films was detached from the egg membrane. For the experiment, an egg membrane was extracted and treated using a previously known method [13]. A $2 \times 2\ cm^2$ of the prepared bio-adhesive film of AmB was cut and pressed against the treated egg membrane for 1 min, and then the other side of the membrane was fixed on a glass slide. The whole assembly was introduced into the dissolution vessel, which had a simulated saliva pH 6.8 dissolution medium preheated at 37 ± 0.5 °C. The system was agitated at 50 rpm. The time (n = 3) for complete dissolution or detachment of the film from the egg membrane was noted.

2.15. *Molecular docking*

Docking of molecules was conducted on Molecular Operating Environment (MOE version 2022.09) [14]. The chemical structures of amphotericin B (PubChem CID: 5280965), and glycerol (PubChem CID: 753) were taken from PubChem, while chemical structures of sodium alginate (β-D-mannuronic acids (M) and α-L-glucuronic (G), linearly linked by 1–4 glycosidic bond) [15], carboxymethyl cellulose [16], and gelatin [17] were drawn on MOE as suggested in the literature. All these molecules were imported into MOE database of compounds and converted into three dimensional form by energy minimization process with default parameters (RMS gradient of 0.5 kcal/mol/Å, and AMBER10:EHT force field). During minimization, MOE automatically add hydrogen atoms to the molecules and simultaneously calculates partial charges on each atom of molecule according to the defined force field. We applied MOE's default docking parameters (triangle matcher placement method and London dG scoring method) with 100 poses of each docked molecule. Amphotericin B was selected as receptor, on which each molecule (glycerol, sodium alginate, carboxymethyl cellulose, and gelatin) was docked separately and the complex was generated. The best docked conformation of molecules was selected according to their docking scores. The atomic interactions between each molecule were visualized by MOE interface.

2.16. *Statistical analysis*

In this study, the data are presented as the mean and standard deviation (SD), derived from three separate evaluations. Statistical

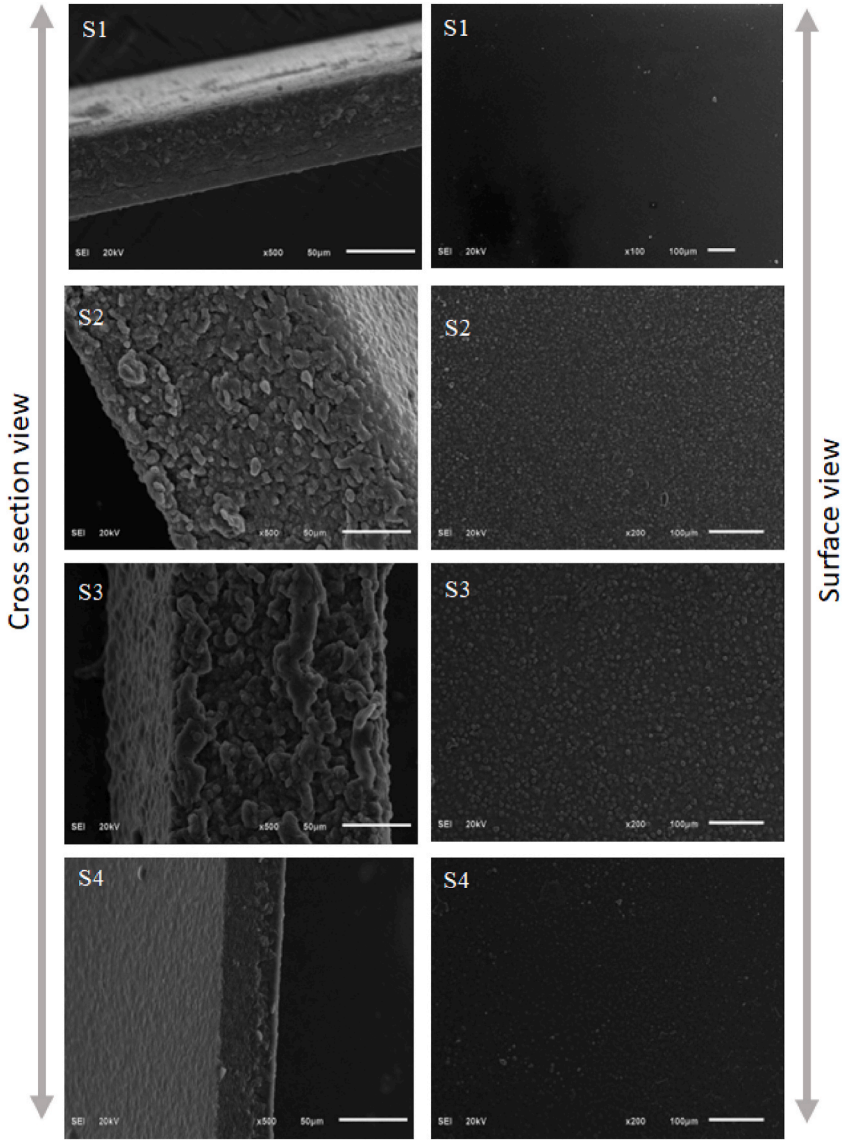

Fig. 2. Scanning electron micrograph for the surface morphology and cross sectional view. Film-S1: control film (no Gly), Film-S2: Gly (0.5 % v/v) film, Film-S3: Gly (1 % v/v) film, and Film-S4: Gly (1.5 % v/v) film.

analysis was performed using a one-way analysis of variance (ANOVA), and Duncan's multiple range test was applied for post-hoc comparisons, considering a significance level of 5 %.

3. Results and discussion

3.1. Visual assessment

Visual assessment of the bioadhesive films was performed to evaluate physical parameters such as difficulty or ease of peeling, endurance, flexibility, adhesiveness, transparency, color, strength, brittleness, etc. The present finding showed in Fig. 1 (S1–S4) display a difference in the transparency, as AmB-loaded films showed a yellowish appearance. It was found that an increase in the concentration of glycerol (Gly) in S2–S4 resulted in the development of homogeneous, adhesive, and flexible yellow transparent films (Fig. 1). The homogeneous, transparent, and flexible films indicated that mixing was effective for developing homogenous plasticized films. Adhesiveness increased possibly because of the movement of glycerol to the surface, via an exudation event as mentioned in a previous report [18].

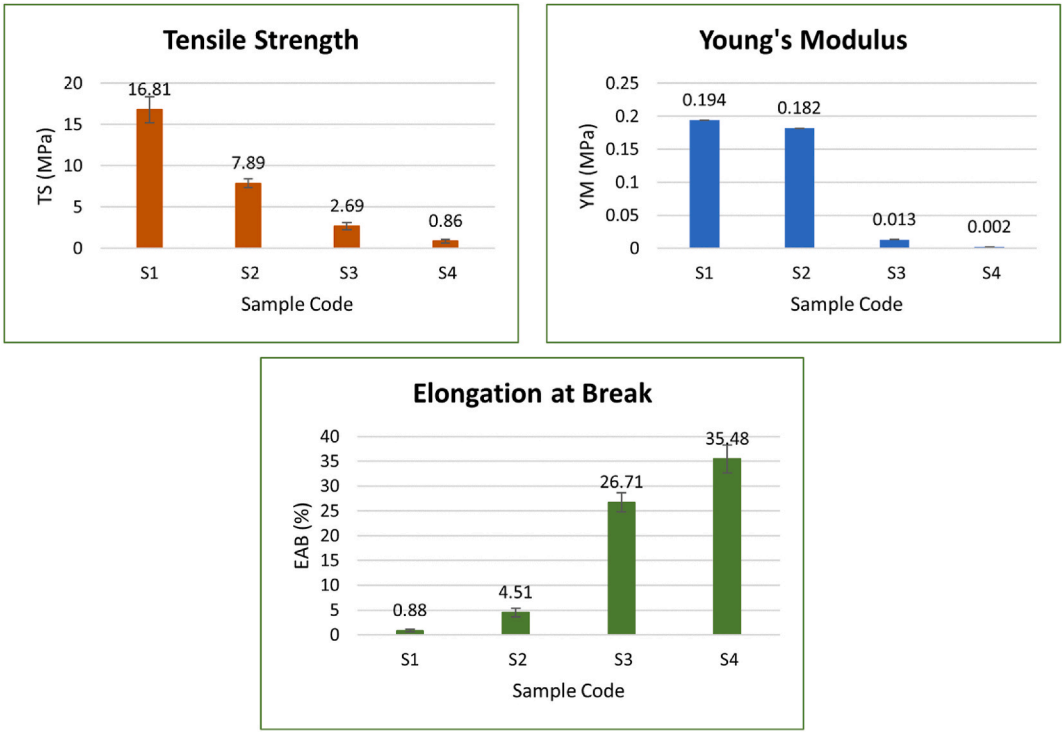

Fig. 3. Tensile strength (TS), Young's Modulus (YM), and Elongation at break (EAB). Film-S1: control film (no Gly), Film-S2: Gly (0.5 % v/v) film, Film-S3: Gly (1 % v/v) film, and Film-S4: Gly (1.5 % v/v) film.

3.2. SEM analysis

Fig. 2(S1–S4) displays the surface and cross-sectional microstructure of the blank, S1 (without AmB and Tween 80) and AmB and Tween 80 film samples (S3–S4). The blank film showed a smooth, homogeneous, and continuous surface with the appearance of minute particles deposited on the film perhaps due to the insolubilized polymeric aggregates, with cracks being observed in the cross-sectional view. Incorporation of the AmB in the S2–S4 samples resulted in the loss of smooth, homogeneous, and continuous surface morphology, and the appearance of granulated structures was observed. These granulated structures may represent the drug precipitated during preparation. S4 samples at the highest Gly concentration showed a less granulated structure. This may be due to a better distribution/dissolution of AmB in this matrix at the highest concentration of Gly. Remnants of the drug still appeared in the S4 samples. The viscosity varied with the addition of Gly whereas the surface properties and solubility varied by the addition of Tween 80. The leftover remnants probably due to either polymer were not restructured or drug aggregates as reported in a previous study [18].

3.3. Mechanical analysis

The study of the mechanical properties (tensile strength (TS), elongation at break (EAB) and Young's modulus (YM)) of the material used for topical application is essential for determining the structural integrity of the bioadhesive films. The findings of this study are shown in Fig. 3(S1–S4). A significant decrease in TS and YM values with the addition of Gly was observed, however, EAB showed a significant increase in sample S1–S4. These findings demonstrate associations between the mechanical strength of the material and the amount of plasticizer used. These results are in agreement with previous findings [19]. Similar results were observed for alginate [18], starch [20,21], and chitosan [22] based films. Similarly, Gly concentration increase resulted in a significant decrease in the tensile strength, whereas the EAB of legume protein-based films increased [23]. However, Gly addition increased the TS of *Eucheuma cottonii* waste seaweed biodegradable films [24]. The decrease in tensile strength and Young's modulus could be linked to an increase in water content with an increase in Gly [18,25].

EAB increased from 0.88 % to 35.45 % with the addition and increase in Gly concentration. When compared to the tensile properties of other biopolymers, such as proteins, plasticized composite films fabricated in the present study possessed less tensile properties [26]. These results are in agreement with an earlier study, where an increase in Gly concentration negatively influenced the tensile strength and elastic modulus of citron peel pectin and alginate films [18,27]. This could be due to the chemical structure difference, variation in the composition of the material, preparation, and storage conditions of the films. Furthermore, this could be due to the change in crystallinity and structural rearrangement caused by the addition of AmB and Gly.

Table 2
Water vapor permeability (WVP), thickness and moisture content of the SA-GE-CMC based AMB films.

Sample Code	WVP (((g*mm)/(m2*h*kPa)))	Thickness (mm)	Moisture content (%)
S1	0.187 ± 0.003^{a}	0.032 ± 0.008^{a}	17.53 ± 0.57^{a}
S2	0.225 ± 0.004^{b}	0.038 ± 0.008^{a}	18.67 ± 0.66^{a}
S2	0.303 ± 0.023^{c}	0.048 ± 0.008^{b}	35.61 ± 0.37^{b}
S4	0.334 ± 0.011^{c}	0.065 ± 0.006^{c}	41.76 ± 1.86^{c}

Values with different superscript letters in each row are significantly different ($P < 0.05$).

Table 3
Color attributes and transparency of the SA-GE-CMC based AMB films.

Codes	L	a*	b*	ΔE	Transmittance (%)
S1	99.74 ± 0.15^{a}	-0.06 ± 0.02^{a}	1.13 ± 0.16^{a}	1.04 ± 0.17^{a}	76.45 ± 1.63^{a}
S2	99.01 ± 0.16^{b}	-1.11 ± 0.11^{b}	5.44 ± 0.17^{b}	7.08 ± 0.66^{b}	45.47 ± 4.01^{b}
S3	98.84 ± 0.13^{b}	-1.62 ± 0.19^{c}	6.42 ± 0.26^{c}	7.74 ± 0.49^{b}	31.13 ± 0.98^{c}
S4	97.42 ± 1.14^{c}	-2.12 ± 0.13^{d}	6.70 ± 0.40^{c}	8.09 ± 0.60^{b}	18.85 ± 0.41^{d}

Values with different superscript letters in each row are significantly different ($P < 0.05$).
L: lightness, a*: green-red color, b*: blue-yellow color, ΔE*: overall color variation.

3.4. Water vapor permeability (WVP) study

The increase in the concentration of Gly resulted in an increase in WVP (Table 2). Our findings indicate that the Gly addition may increase the free volume between the polymeric chains and, reduce the density of the material thereby encouraging the diffusion of water vapor [28]. The present results are in agreement with previous findings where the WVP of cassava native starches, arrowroot starch, Malva sylvestris flower gum, and maize starch/PVOH/chitosan-based films increased with increasing Gly amount [29–32]. In an earlier report, the WVP of edible film fabricated from cress seed carbohydrate gum increased as the Gly amount increased from 25 % to 50 % w/w in the formulation causing improvement of the film's flexibility with an increase in the elongation at break, and a significant decrease in tensile strength [33].

3.5. Moisture content of the films

Generally, the hydrophilicity of polymeric films increases with increasing concentration of plasticizers. In our study with increasing concentration of Gly (0.5–1.5 % (v/v or w/w) increment in the moisture content from 17.53 % to 41.76 % of the films were observed (Table 2). This plasticizer-dependent increase in the moisture content of hydrocolloid films has been reported in previous studies. An increase in Gly concentration caused an increase in the water retention in the film, which was due to the water-holding capacity of plasticizers [30,34,35]. Another report showed that Gly plasticized films usually retained more moisture than sorbitol films, and the tensile strength declined with increasing glycerol content, whereas the elongation at break increased [36].

3.6. Thickness analysis

There was an insignificant difference in the thickness of the blank (S1) and Gly-plasticized films with a 0.5 % concentration of S2 as described in Table 2. An increase in the thickness of the film was observed from 0.038 mm to 0.065 mm in response to an increase in Gly concentrations from 0.5 % to 1.5 %. This could be due to the plasticizer effect in changing and reorganizing intermolecular polymer chain networks, influencing free volumes to make thicker films [37,38].

3.7. Color analysis

Visual characterization, such as the transparency and color of bio-adhesive films plays an important role as it affects patient acceptability. The results showed that the L* value (lightness) reduced with the incorporation of Gly (Table 3). Nevertheless, there was no substantial variation in L* values. The a* (-0.06 to -2.12) and b* (1.13 to 6.70) values of the samples showed significant color variation between the blank (S1) and drug-loaded samples (S2–S4). The addition of AMB increased the yellowness of the films, thus, the b* value of S2 may be greater than S1 [39]. The transmittance (%) values for films with 0.5 %, 1 %, and 1.5 % of Gly were 45.4 %, 31.13 %, and 18.85 %, respectively, indicating a considerable decrease in transmittance with Gly addition (Table 3). These results indicate that the addition of Gly increased the opacity of the material, demonstrating its ability to act as a shield against UV rays [40, 41]. This increase in opacity with the addition of Gly could be due to the distribution of glycerol drops across the films, resulting in a breakdown of the film structure [40].

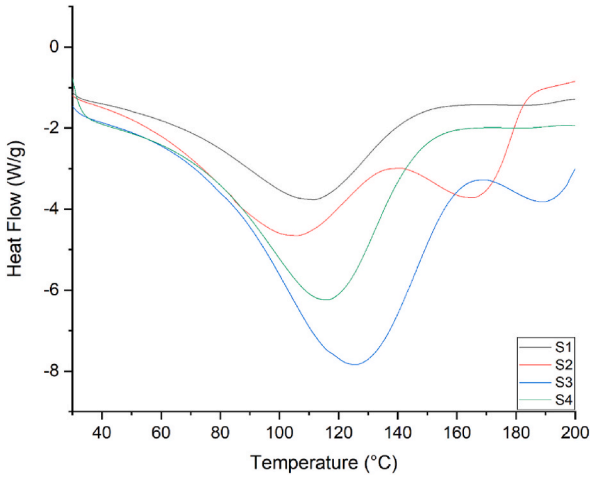

Fig. 4. DSC analysis of SA-GE-CMC based bioadhesive films (S1–S4). Film-S1: control film (no Gly), Film-S2: Gly (0.5 % v/v) film, Film-S3: Gly (1 % v/v) film, and Film-S4: Gly (1.5 % v/v) film.

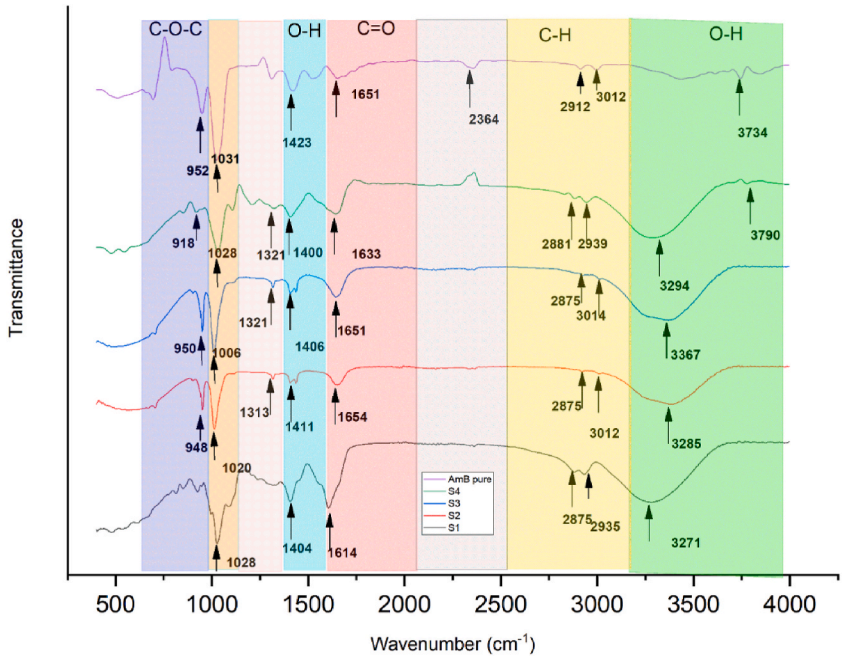

Fig. 5. FTIR analysis of bioadhesive films (S1–S4). Film-S1: control film (no Gly), Film-S2: Gly (0.5 % v/v) film, Film-S3: Gly (1 % v/v) film, and Film-S4: Gly (1.5 % v/v) film.

3.8. DSC analysis

Bioadhesive films must be thermally resistant to withstand the changes in the temperature of the external environment. DSC analysis was performed to assess the thermal behavior of AmB-loaded bioadhesive film. Fig. 4(S1–S4) shows DSC curves between 0 and 200 °C. The DSC thermograms of all films showed broad endothermic peaks at various temperature ranges. The endothermic peak of the blank film without AmB appeared at 110.8 °C (T1). The addition of Gly and AmB resulted in the formation of two endothermic peaks in each S2 (T1≈ 104.5 °C, T2≈ 166.78 °C), and S3 samples (T1≈ 125 °C, T2≈ 190 °C), respectively. However, the S4 sample showed only one endothermic peak (T1≈ 115.3 °C) like S1 (T1≈ 110.8 °C). The increase in the concentration of Gly resulted in an increase in the endothermic temperatures from S2 (T1≈ 104.5 °C) to S4 (T1≈ 115.3 °C). In addition, the endothermic temperature (T2) from S2 (T2≈ 166.78 °C) to S3 (T2≈ 190 °C) increased. The appearance of two endothermic characteristic peaks in the DSC of the S2 and S3 samples could be due to the presence of AmB, as reported in the literature [41]. In previous studies, two characteristic endothermic peaks were observed for AmB at 168.5 and 213.4 °C However, the complete disappearance of the characteristic peaks for

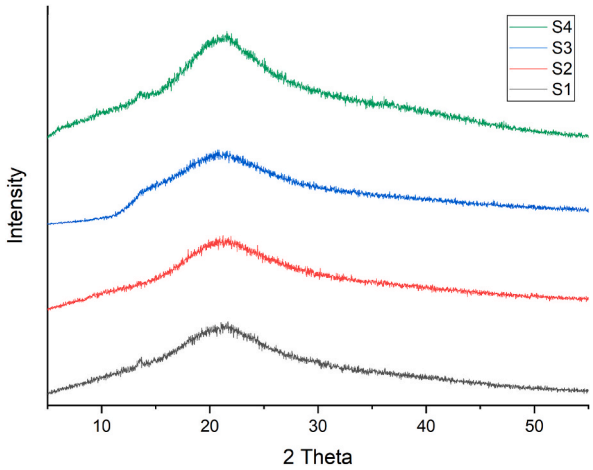

Fig. 6. XRD diffractogram of bioadhesive films (S1–S4). Film-S1: control film (no Gly), Film S2: Gly (0.5 % v/v) film, Film-S3: Gly (1 % v/v) film, and Film-S4: Gly (1.5 % v/v) film.

AmB from the thermograms of S4 (Fig. 4) indicated the loss of the crystalline lattice of the drug and formation of an amorphous state as a result of the inclusion of the drug inside the polymers [41–43]. The apparent cause behind the increase in the endothermic peak temperature with glycerol proportion is not clear but may be associated with changes in the crystallinity of the film matrix, as confirmed by XRD. Sun et al., 2017 demonstrated a higher degree of crystallinity in a polymeric matrix presents higher thermal stability of the film [44]. A previous report demonstrated an endothermic peak in the DSC of a pure SA edible film at 134.39 ± 2.64 °C due to such phase transitions (because of the melting of the sample) [45]. Another report showed that the decomposition temperature of pure SA is 251.12 °C [46].

In an earlier report, the DSC thermogram of AmB showed a sharp endothermic peak at 174 °C, corresponding to its melting point, suggesting a crystalline nature, followed by a glass transition temperature (Tg) at T = 200 °C [43]. In another report, the DSC thermogram of crystalline AmB presented two broad endothermic peaks at 80.40 °C and 166.18 °C corresponding to the moisture loss, and the melting point, respectively [47]. Another report showed DSC thermograms of the pure GE films showing two sharp endothermic peaks at 104.50 °C and 225.03 °C [48].

3.9. FTIR analysis

Infrared spectroscopy can be employed to study the interactions among biopolymers, plasticizers, and drugs, highlighting any alterations in the drug composition within the films relative to its pure form. Fig. 5(S1–S4) presents the FTIR spectra of the pure AmB drug, the control sample SA-GE-CMC-GLY (S1), and the AmB-SA-GE-CMC-GLY composite (S2–S4). All samples exhibited wide bands within the 3000–3600 cm^{-1} range, which is attributed to the O–H group's stretching vibrations found in SA, CMC, and Gly. It was observed that the FTIR spectra for pure AmB significantly varied from the composite samples (S2–S4). The pure AmB spectra displayed distinctive sharp bands at 3734 cm^{-1}, indicative of the NH stretch band, and at 2912 cm^{-1}, 3012 cm^{-1}, 1651 cm^{-1}, and 1031 cm^{-1}, corresponding to CH stretching, the carbonyl group, and AmB, respectively, as visualized in Fig. 5. This variation is attributed to the interactions of AmB with the polymers and the plasticizer. Moreover, the absence of the AmB's specific peak at 1549 cm^{-1} in the S2–S4 samples indicates the development of a robust electrostatic bond between the polymer and the drug [47,49–51]. The band ranging from 2875 to 3012 cm^{-1} is indicative of the C–H stretching vibrations. Bands observed at 1614–1654 cm^{-1} and 1400–1411 cm^{-1} correspond to the asymmetric and symmetric stretching vibrations of the C═O and COO- groups, respectively. Additionally, the band within 1006–1028 cm^{-1} is associated with the ring stretching vibrations of C–O and C–O. Notable peaks at approximately 3367 cm^{-1}, resulting from NH stretching, 1654 cm^{-1} from the amide C═O, and 1321 cm^{-1} from C–N stretching, are primarily attributed to the presence of GE. The bands found between 918 and 950 cm^{-1} in samples S2–S4 are likely due to the C–O stretching vibrations from both the plasticizer and the polysaccharide. A pronounced absorption peak within the 1633–1654 cm^{-1} range may be linked to the hydroxyl group from the water retained in the film [52,53].

Typically, films require plasticization because the softening effect from water isn't sustainable in solid forms like films, given that water eventually evaporates. Hence, to counteract this rigidity, it's often recommended to introduce plasticizers, like Gly. These agents enhance film flexibility by diminishing intermolecular hydrogen bonding, effectively increasing the space between molecules [54]. In this study, for the plasticized films labeled S2–S4, peaks were detected around 3294 cm^{-1} and 1028 cm^{-1}. These peaks can be attributed to the O–H stretching vibrational groups of glycerol and either O–H deformation or C–O stretching vibrations. Analogous peaks were also identified in the blank film (S1) [30].

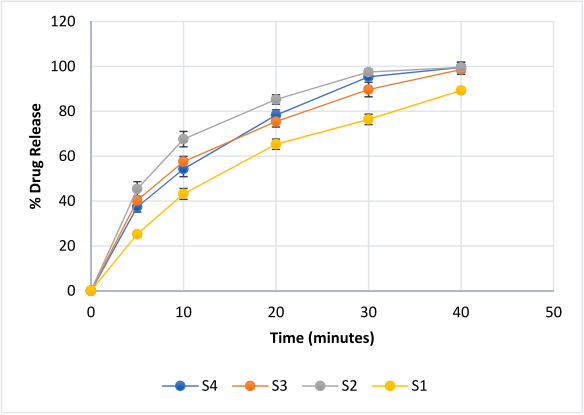

Fig. 7. *In-vitro* drug release of AmB formulations in simulated saliva, pH 6.8 conditions. Film-S1: control film (no Gly), Film-S2: Gly (0.5 % v/v) film, Film-S3: Gly (1 % v/v) film, and Film-S4: Gly (1.5 % v/v) film.

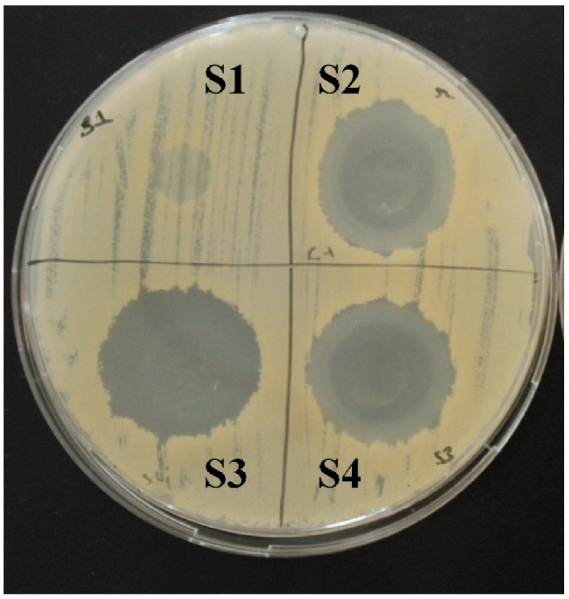

Fig. 8. *Candida albicans* zone of inhibition (included with disc diameter of 10 mm). Film-S1: control film (no Gly), Film-S2: Gly (0.5 % v/v) film, Film-S3: Gly (1 % v/v) film, and Film-S4: Gly (1.5 % v/v) film.

3.10. XRD analysis

The X-ray diffractograms of all the samples showed a broad peak at 21° (Fig. 6). Films S1 and S4 showed characteristic peaks at 13.57°, which could be attributed to the presence of SA [55]. Fig. 6(S1–S4) shows the XRD analysis of the samples (S1–S4). The XRD findings revealed a significant variation in the crystallinity and amorphousness of the films when compared to the blank sample. The X-ray diffractogram of the blank sample showed a small peak at $2\theta \approx 13.57°$ and a broad diffraction peak at $2\theta \approx 21°$, suggesting low crystallinity [56]. An increase in the crystallinity from S1 to S3 was observed from $2\theta \approx 14.6°$ to $2\theta \approx 21.9°$, however, the crystallinity further decreased in S4 ($2\theta \sim 16.4°$). It was evident that the crystallinity of the composite films increased with the addition of Gly [34]. The crystallinity was calculated using the software (Diffract Eva software package) and the following order of crystallinity was obtained:

$$S3 > S2 > S4 > S1$$

This could be because of Gly interfering with intermolecular interactions between the polymers, thus influencing the regularity, and close packing of polymers to form crystalline structures. Moreover, this may be because of Gly on the intermolecular interactions between SA, GE, and AmB, making the composite films more crystalline than the blank. In previous studies, it was reported that the crystallinity of the kudzu starch-based, cassava starch and sugar palm starch-based films was enhanced as Gly concentration increased

Table 4
Antimicrobial activity of GE-SA films incorporated with AMB against test microorganisms.

Sample code	Inhibitory zone (mm^2)
S1	10.26 ± 0.351^{a}
S2	23.56 ± 0.766^{b}
S3	22.72 ± 1.33^{b}
S4	24.49 ± 2.19^{b}

Values with different superscript letters in each row are significantly different ($P < 0.05$).

[34,57,58].

3.11. In-vitro drug release

The drug release studies showed an increase in the drug release kinetics as the concentration of plasticizers increased (S4>S3>S2), as compared to the formulation without the plasticizer (S1). This showed that the concentration of the plasticizer has a substantial role in the release of the drug probably due to the improved mechanical properties and flexibility of the films (Fig. 7(S1–S4)). Our results were supported by a previous study that claims to have a direct relationship between increasing plasticizer concentrations with increasing drug release [59]. The drug content for all the formulations was found to be 0.99 ± 0.122 mg. All the formulations with plasticizer (S2, S3, S4) showed a burst release as compared to the S1 (without plasticizer). $T_{90\ \%}$ drug release for S1 (>40 min), S2 (28.20 min), S3 (30.10 min), and S4 (27.70 min), which again emphasized that the increasing concentration of the plasticizer results in an increase in the drug release from the formulation. This behaviour can be attributed to the increase in flexibility of polymeric matrix. This increased mobility of the polymer chains can facilitate the diffusion of the drug through the composite films.

3.12. In-vitro bioadhesion time

The results of the *in-vitro* bioadhesion times (2.32 ± 1.03 min) for all the formulations showed the strong adhesive nature of the prepared film to the substrate. The results also emphasize the importance of a strong bioadhesion of the films to have a good release profile. Our results of bioadhesion time are in line with a previously conducted study [60].

3.13. Antimicrobial assay against C. albicans

The antimicrobial assay of AMB loaded films was carried out against *Candida albicans* and the results are represented in Fig. 8 (S1–S4). SI blank composite films did not show any antimicrobial activity against the test organism. The diameters of the inhibition zones for the AMB loaded films against *C. albicans* were in the range of 23.56 ± 0.766 to 24.49 ± 2.19 mm. Table 4 shows the antifungal activity of the films against *C. albicans*. A maximum growth inhibition zone of 24.49 mm was obtained with S4 sample, however AMB loaded samples showed insignificant ($P \geq 0.05$) difference between ZOI.

In accordance to reported study, there are several classes of antimicrobial activity of the polymer based films depending on the diameter of zone of inhibition (ID). If ID < 17 mm, the films are consider insensitve; 18–23 mm ID indicates sensitivity of the films, ID between 24 and 28 mm is considered very sensitive and ID > 29 mm is considered extremely sensitive [61]. According to the current results, it can be observed that the AMB loaded show ID between 24 and 28 mm and the strain is sensitive to the formulated films. Similar inhibition activity of AMB was reported in a previous paper against *C. albicans* and *A. niger* [62].

3.14. Docking analysis

The inter-molecular interactions between AmB, sodium alginate, gelatin, glycerol and carboxymethyl cellulose were further predicted through *in-silico* docking experiments. The hydroxyl moieties of CMC shows excellent hydrogen bonding with the ring oxygen (2.02 Å) and one of the hydroxyl groups (2.22 Å) of AmB with docking score of −4.95 kcal/mol. The binding mode analysis of sodium alginate reflects that one of its carboxyl group binds with the –OH of AmB through H-bond (2.06 Å) with docking score of −5.92 kcal/mol, however, SA also has a chance of creating ionic bond with the sodium methoxy acetate group of CMC. The docking score of SA-AmB complex is higher than the docking score of SA-CMC complex (−5.20 kcal/mol). SA molecule also showed intramolecular interaction between its –OH and the acetate moieties (1.84 Å). When gelatin was docked, interestingly it did not bind directly with AmB, however gelatin created a mash of interactions with CMC and SA, and the conformation of AmB is interlocked between CMC and gelatin. The docking score of AmB-CMC-SA-Gelatin complex is −6.86 which is highly negative because of its greater potential for complex formation with CMC and SA. The guanidium moiety of gelatin formed multiple hydrogen bonds with the acetate group (2.01 Å and 2.02 Å) and ring oxygen (2.24 Å) of SA. Whereas the same guanidinium group of gelatin formed intermolecular H-bond with the acetate moiety of gelatin (1.95 Å). Moreover, two of the amide groups of gelatin generates H-bond and an ionic interaction with the sodium methoxy oxo propanolate group of CMC at a distance of 2.43 Å and 2.74 Å, respectively. When the glycerol molecule was docked in AmB-CMC-SA-Gelatin complex to see the binding preference of glycerol, this molecule exclusively binds with the –OH (2.07

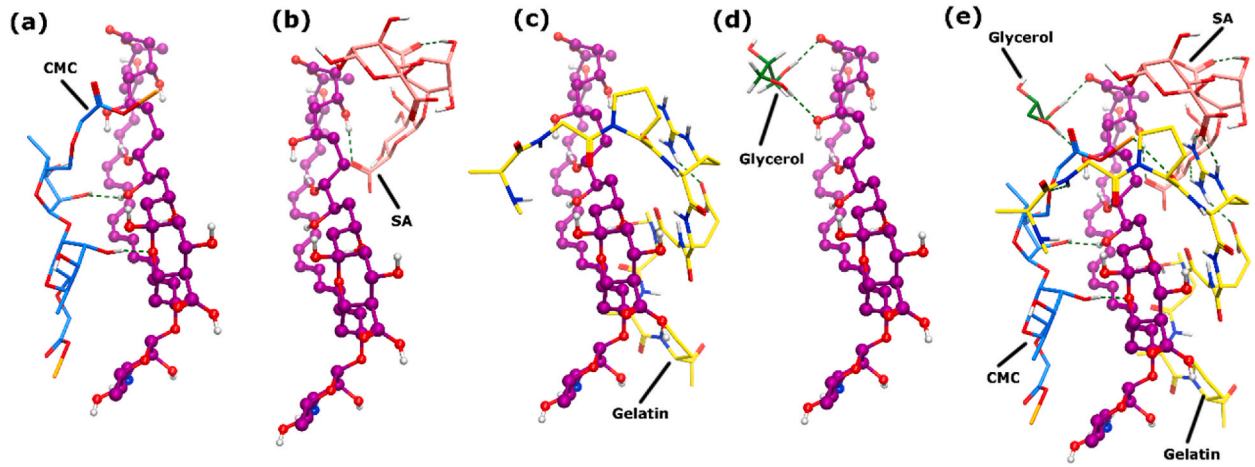

Fig. 9. The binding modes of (a) CMC (b) SA (c) Gelatin (d) Glycerol is shown with the AmB (depicted in magenta ball and stick model). (E). The complex between AmB and CMC-SA-Gelatin-Glycerol is shown. H-bonds are presented in green dotted lines. (For interpretation of the references to color in this figure legend, the reader is referred to the Web version of this article.)

Å) and acetate (2.03 Å) moieties of AmB with docking score of −3.53 kcal/mol and did not show interaction with CMC, SA, and gelatin molecules. It indicates that this small molecule of glycerol is stabilizing the interlocking of AmB between CMC and gelatin. The binding modes of these molecules are shown in Fig. 9(a–e).

4. Conclusion

In conclusion, the current research investigated the effect of glycerol, functioning as a plasticizer, on the properties of bioadhesive films comprising sodium alginate (SA) and gelatin (GE) polymers incorporated with amphotericin B (AmB). An upward trend in glycerol concentration correlated with increased water vapor permeability (WVP), elongation at break (EAB), film thickness, and moisture content, suggesting enhanced film flexibility and resistance to water vapor transmission. Conversely, there was a decline in transparency, tensile strength (TS), and Young's modulus (YM) with the rise in glycerol levels. Fourier Transform Infrared (FTIR) spectroscopy analysis revealed the presence of intermolecular hydrogen bonds between glycerol and the polymer matrix in these plasticized films, demonstrating the interactive synergy and compatibility among the constituents. Additionally, the AmB-loaded films exhibited significant antimicrobial efficacy against *Candida albicans*. Docking is an important strategy to predict the molecular binding between two molecules at atomic level. The docking results in this study also reflect that glycerol is stabilizing the formation of complex between AmB and CMC and gelatin by particularly interacting with AmB. These results indicate that employing glycerol as a plasticizer in this specific polymeric mixture is a promising approach for the effective formulation of bioadhesive films.

Funding source

The study was supported by The Research Council, Oman grant number BFP/URG/HSS/22/127 and BFP/RGP/HSS/22/007.

Institutional review board statement

This study does not contain any studies with human or animal subjects performed by any of the authors.

Data availability statement

Not applicable.

CRediT authorship contribution statement

Saurabh Bhatia: Writing – review & editing, Writing – original draft, Conceptualization. **Ahmed Al-Harrasi:** Supervision, Conceptualization. **Ibrahim Hamza Almohana:** Methodology, Conceptualization. **Mustafa Safa Albayati:** Methodology. **Muhammad Jawad:** Writing – review & editing, Writing – original draft. **Yasir Abbas Shah:** Methodology. **Sana Ullah:** Software, Methodology. **Anil K. Philip:** Writing – review & editing, Writing – original draft. **Sobia Ahsan Halim:** Writing – original draft, Software. **Ajmal Khan:** Writing – review & editing. **Md Khalid Anwer:** Data curation. **Esra Koca:** Methodology, Formal analysis. **Levent Yurdaer Aydemir:** Writing – review & editing, Formal analysis. **Sevgin Dıblan:** Methodology.

Declaration of competing interest

The authors declare no financial interests/personal relationships which may be considered as potential competing interests.

Acknowledgments

The authors are thankful to the Natural and Medical Sciences Research Center, University of Nizwa, Oman for providing research facilities to conduct the current study.

References

[1] F. Bongomin, et al., Global and multi-national prevalence of fungal diseases—estimate precision, Journal of fungi 3 (4) (2017) 57.
[2] L. Scorzoni, et al., Antifungal therapy: new advances in the understanding and treatment of mycosis, Front. Microbiol. 8 (2017) 36.
[3] A. Noor, C.V. Preuss, Amphotericin B (2018).
[4] L.-L.R. Cabrales-Vargas, R. Laniado-Laborín, Amphotericin B: side effects and toxicity, Rev. Iberoam. De. Micol. 264 (2009) 223–227.
[5] K. Pamlényi, et al., Formulation and optimization of sodium alginate polymer film as a buccal mucoadhesive drug delivery system containing cetirizine dihydrochloride, Pharmaceutics 13 (5) (2021) 619.
[6] V. Kanikireddy, et al., Carboxymethyl cellulose-based materials for infection control and wound healing: a review, Int. J. Biol. Macromol. 164 (2020) 963–975.
[7] M.E. Lane, Skin penetration enhancers, Int. J. Pharm. 447 (1–2) (2013) 12–21.
[8] S. Kim, K.B. Song, Antimicrobial activity of buckwheat starch films containing zinc oxide nanoparticles against Listeria monocytogenes on mushrooms, Int. J. Food Sci. Technol. 53 (6) (2018) 1549–1557.
[9] B.G. Erdem, S. Dıblan, S. Kaya, Development and structural assessment of whey protein isolate/sunflower seed oil biocomposite film, Food Bioprod. Process. 118 (2019) 270–280.
[10] J. Zhao, Y. Wang, C. Liu, Film transparency and opacity measurements, Food Anal. Methods 15 (10) (2022) 2840–2846.
[11] K.-H. Seol, et al., Antimicrobial effect of κ-carrageenan-based edible film containing ovotransferrin in fresh chicken breast stored at 5 C, Meat Sci. 83 (3) (2009) 479–483.
[12] E. Matuschek, D.F. Brown, G. Kahlmeter, Development of the EUCAST disk diffusion antimicrobial susceptibility testing method and its implementation in routine microbiology laboratories, Clin. Microbiol. Infection 20 (4) (2014) O255–O266.
[13] A.K. Philip, N. Singh, K. Pathak, Egg shell membrane as a substrate for optimizing in vitro transbuccal delivery of glipizide, Pharmaceut. Dev. Technol. 14 (5) (2009) 540–547.
[14] Moe, Molecular Operating Environment Version 2014.09; Chemical Computing Group, Canada, Montreal, QC, 2014.
[15] O.D. Frent, et al., Sodium alginate—natural microencapsulation material of polymeric microparticles, Int. J. Mol. Sci. 23 (20) (2022) 12108.
[16] M.S.A. Rani, et al., Biopolymer electrolyte based on derivatives of cellulose from kenaf bast fiber, Polymers 6 (9) (2014) 2371–2385.
[17] S. Kommareddy, D.B. Shenoy, M.M. Amiji, Gelatin Nanoparticles and Their Biofunctionalization, Nanotechnologies for the life sciences, Online, 2007.
[18] C. Gao, E. Pollet, L. Avérous, Properties of glycerol-plasticized alginate films obtained by thermo-mechanical mixing, Food Hydrocolloids 63 (2017) 414–420.
[19] V. Jost, et al., Influence of plasticiser on the barrier, mechanical and grease resistance properties of alginate cast films, Carbohydr. Polym. 110 (2014) 309–319.
[20] L. Averous, N. Boquillon, Biocomposites based on plasticized starch: thermal and mechanical behaviours, Carbohydr. Polym. 56 (2) (2004) 111–122.
[21] A. Farahnaky, B. Saberi, M. Majzoobi, Effect of glycerol on physical and mechanical properties of wheat starch edible films, J. Texture Stud. 44 (3) (2013) 176–186.
[22] M. Matet, et al., Innovative thermoplastic chitosan obtained by thermo-mechanical mixing with polyol plasticizers, Carbohydr. Polym. 95 (1) (2013) 241–251.
[23] E.J. Hopkins, et al., Effect of glycerol on the physicochemical properties of films based on legume protein concentrates: a comparative study, J. Texture Stud. 50 (6) (2019) 539–546.
[24] S. Hidayati, Zulferiyenni, U. Maulidia, W. Satyajaya, S. Hadi, Effect of Glycerol Concentration and Carboxy Methyl Cellulose on Biodegradable Film Characteristics of Seaweed Waste, Heliyon, 2021.
[25] S.P. Cabello, et al., New bio-polymeric membranes composed of alginate-carrageenan to be applied as polymer electrolyte membranes for DMFC, J. Power Sources 265 (2014) 345–355.
[26] J. Zink, et al., Physical, chemical and biochemical modifications of protein-based films and coatings: an extensive review, Int. J. Mol. Sci. 17 (9) (2016) 1376.
[27] W.A. Asfaw, K.D. Tafa, N. Satheesh, Optimization of citron peel pectin and glycerol concentration in the production of edible film using response surface methodology, Heliyon 9 (3) (2023).
[28] F. Bi, et al., Development of active packaging films based on chitosan and nano-encapsulated luteolin, Int. J. Biol. Macromol. 182 (2021) 545–553.
[29] Y.D. Adjouman, et al., Water vapor permeability of edible films based on improved Cassava (Manihot esculenta Crantz) native starches, J. Food Process. Technol. 8 (2017).
[30] J. Tarique, S. Sapuan, A. Khalina, Effect of glycerol plasticizer loading on the physical, mechanical, thermal, and barrier properties of arrowroot (Maranta arundinacea) starch biopolymers, Sci. Rep. 11 (1) (2021) 13900.
[31] C. Caicedo, et al., Effect of plasticizer content on mechanical and water vapor permeability of maize starch/PVOH/chitosan composite films, Materials 15 (4) (2022) 1274.
[32] Z. Jaderi, et al., Effects of glycerol and sorbitol on a novel biodegradable edible film based on Malva sylvestris flower gum, Food Sci. Nutr. 11 (2) (2023) 991–1000.
[33] M. Jouki, et al., Effect of glycerol concentration on edible film production from cress seed carbohydrate gum, Carbohydr. Polym. 96 (1) (2013) 39–46.
[34] M.L. Sanyang, et al., Effect of plasticizer type and concentration on physical properties of biodegradable films based on sugar palm (Arenga pinnata) starch for food packaging, J. Food Sci. Technol. 53 (2016) 326–336.
[35] M. Ghasemlou, F. Khodaiyan, A. Oromiehie, Physical, mechanical, barrier, and thermal properties of polyol-plasticized biodegradable edible film made from kefiran, Carbohydr. Polym. 84 (1) (2011) 477–483.
[36] S. Faust, et al., Effect of glycerol and sorbitol on the mechanical and barrier properties of films based on pea protein isolate produced by high-moisture extrusion processing, Polym. Eng. Sci. 62 (1) (2022) 95–102.
[37] S.M.A. Razavi, A.M. Amini, Y. Zahedi, Characterisation of a new biodegradable edible film based on sage seed gum: influence of plasticiser type and concentration, Food Hydrocolloids 43 (2015) 290–298.
[38] M. Sanyang, et al., Development and characterization of sugar palm starch and poly (lactic acid) bilayer films, Carbohydr. Polym. 146 (2016) 36–45.
[39] P. Chennell, et al., Do ophthalmic solutions of amphotericin B solubilised in 2-Hydroxypropyl-γ-Cyclodextrins possess an extended physicochemical stability? Pharmaceutics 12 (9) (2020) 786.
[40] P. Zhang, Y. Zhao, Q. Shi, Characterization of a novel edible film based on gum ghatti: effect of plasticizer type and concentration, Carbohydr. Polym. 153 (2016) 345–355.
[41] L. Cao, W. Liu, L. Wang, Developing a green and edible film from Cassia gum: the effects of glycerol and sorbitol, J. Clean. Prod. 175 (2018) 276–282.
[42] B. Al-Quadeib, et al., Stealth amphotericin B nanoparticles for oral drug delivery: in vitro optimization, Saudi Pharm. J 23 (2015) 290–302.
[43] N.A.H. Al-Assady, E. Saad, I. Alrubayae, Preparation, characterization and evaluation of controlled release microspheres containing amphotericin B, Journal of Basrah Researches (Science) 39 (2013) 114–131.

[44] L. Sun, et al., Preparation and characterization of chitosan film incorporated with thinned young apple polyphenols as an active packaging material, Carbohydr. Polym. 163 (2017) 81–91.
[45] J. Kadzińska, et al., Influence of vegetable oils addition on the selected physical properties of apple–sodium alginate edible films, Polym. Bull. 77 (2020) 883–900.
[46] M. Aprilliza, Characterization and properties of sodium alginate from brown algae used as an ecofriendly superabsorbent, in: IOP Conference Series: Materials Science and Engineering, IOP Publishing, 2017.
[47] K. Kaur, P. Kumar, P. Kush, Amphotericin B loaded ethyl cellulose nanoparticles with magnified oral bioavailability for safe and effective treatment of fungal infection, Biomed. Pharmacother. 128 (2020) 110297.
[48] J.C. Nunes, et al., Effect of green tea extract on gelatin-based films incorporated with lemon essential oil, J. Food Sci. Technol. 58 (1) (2021) 1–8.
[49] I. Ali, et al., Preliminary investigation of novel tetra-tailed macrocycle amphiphile based nano-vesicles for amphotericin B improved oral pharmacokinetics, Artif. Cell Nanomed. Biotechnol. 46 (sup3) (2018) 1204–1214.
[50] M. Nahar, N.K. Jain, Preparation, characterization and evaluation of targeting potential of amphotericin B-loaded engineered PLGA nanoparticles, Pharmaceut. Res. 26 (2009) 2588–2598.
[51] B.T. Al-Quadeib, et al., Stealth Amphotericin B nanoparticles for oral drug delivery: in vitro optimization, Saudi Pharmaceut. J. 23 (3) (2015) 290–302.
[52] R. Ilyas, et al., Effect of sugar palm nanofibrillated cellulose concentrations on morphological, mechanical and physical properties of biodegradable films based on agro-waste sugar palm (Arenga pinnata (Wurmb.) Merr) starch, J. Mater. Res. Technol. 8 (5) (2019) 4819–4830.
[53] J.W. Park, S.S. Im, Biodegradable polymer blends of Poly (L-lactic acid) and gelatinized starch, Polym. Eng. Sci. 40 (12) (2000) 2539–2550.
[54] S.P. Bangar, et al., Functionality and applicability of starch-based films: an eco-friendly approach, Foods 10 (9) (2021) 2181.
[55] C. Xiao, et al., Blend Films from Sodium Alginate and Gelatin Solutions, 2001.
[56] S. Bhagyaraj, I. Krupa, Alginate-mediated synthesis of hetero-shaped silver nanoparticles and their hydrogen peroxide sensing ability, Molecules 25 (3) (2020) 435.
[57] Y. Zhong, Y. Li, Effects of glycerol and storage relative humidity on the properties of kudzu starch-based edible films, Starch Staerke 66 (5–6) (2014) 524–532.
[58] P.V.A. Bergo, et al., Physical properties of edible films based on cassava starch as affected by the plasticizer concentration, Packag. Technol. Sci.: Int. J. 21 (2) (2008) 85–89.
[59] P. Jantrawut, et al., Effect of plasticizer type on tensile property and in vitro indomethacin release of thin films based on low-methoxyl pectin, Polymers 9 (7) (2017) 289.
[60] O.Y. Mady, et al., Formulation and bioavailability of novel mucoadhesive buccal films for candesartan cilexetil in rats, Membranes 11 (9) (2021) 659.
[61] M. Pereda, et al., Chitosan-gelatin composites and bi-layer films with potential antimicrobial activity, Food Hydrocolloids 25 (5) (2011) 1372–1381.
[62] A.A. Albadr, et al., Rapidly dissolving microneedle patch of amphotericin B for intracorneal fungal infections, Drug Delivery and Translational Research (2022) 1–13.